Supporting Information

A Novel Mechanism of Controlling Ultramicropore Size in Carbons at Sub-angstrom Level for Molecular Sieving of Propylene/propane Mixtures

Shengjun Du [a], Jiawu Huang [a], Abdul Waqas Anjum [b], Jing Xiao [b]*, Zhong Li [a,b]*

[a] School of Chemistry and Chemical Engineering, South China University of Technology, Guangzhou, PR China
E-mail: cezhli@scut.edu.cn

[b] The Key Laboratory of Enhanced Heat Transfer and Energy Conservation, Ministry of Education, Guangzhou, PR China
E-mail: cejingxiao@scut.edu.cn

Table of Contents

Supporting Figures

Figure. S1 SEM micrographs of SCHs.

Figure. S2 SEM micrographs of Starch-800.

Figure. S3 ^{13}C CP-MAS spectra of SCMS-0.2-800.

Figure. S4 Full survey XPS spectra of starch and Starch-800.

Figure. S5 Deconvolution of C 1s spectra for starch and Starch-800.

Figure. S6 Full survey XPS spectra and deconvolution of C 1s spectra for SCHs.

Figure. S7 Full survey XPS spectra for SCMS-0.2-*y*.

Figure. S8 Deconvolution of C 1s spectra for SCMS-0.2-*y*.

Figure. S9 N_2 adsorption isotherms at 77 K on SCMS-0.05-*y*, SCMS-0.2-*y* and SCMS-1- *y*.

Figure. S10 CO_2 adsorption isotherms at 273 K on Starch-800, SCMS-*x*-800 and SCMS-0.2-*y*.

Figure. S11 C_3H_6 and C_3H_8 adsorption isotherms of Starch-800 at 298 K and 0-1 bar.

Figure. S12 C_3H_6 and C_3H_8 adsorption isotherms of SCMS-0.05-800 and SCMS-1-800 at 298 K and 0-1 bar.

Figure. S13 Surface area plot of SCMS-0.05-800 and SCMS-1-800.

Figure. S14 Surface area plot of SCMS-0.2- *y*.

Figure. S15 C_3H_6 adsorption isotherms of SCMS-0.2-800 at different temperatures and Virial fitting of the C_3H_6 adsorption isotherms.

Figure. S16 Heat of adsorption for C_3H_6 on SCMS-0.2-800.

Figure. S17 Schematic illustration of the apparatus for the gas breakthrough tests.

Figure. S18 Breakthrough cycling test of SCMS-0.2-800.

Figure. S19 C_3H_6 and C_3H_8 adsorption isotherms of SCMS-0.2-800 at high temperature and high pressure.

Supporting Tables

Table S1 Elemental compositions of SCHs from XPS analysis.

Table S2 Summary of separation metrics of top-performing materials for separation of C_3H_6/C_3H_8 based on thermodynamics at 1 bar and 298K.

Table S3 Textural properties of SCMS-0.2-*y* samples.

4. References

Supporting Figures

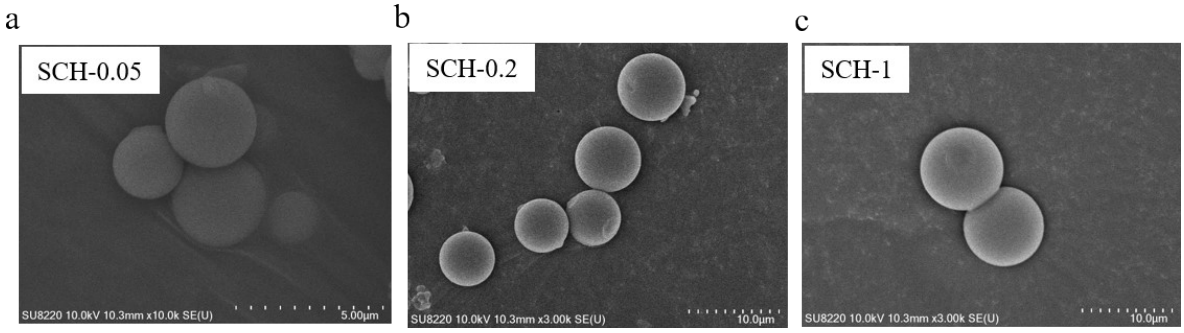

Figure S1. SEM micrographs of SCHs.

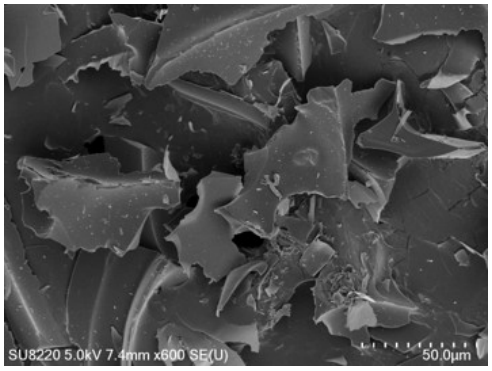

Figure S2. SEM micrographs of Starch-800.

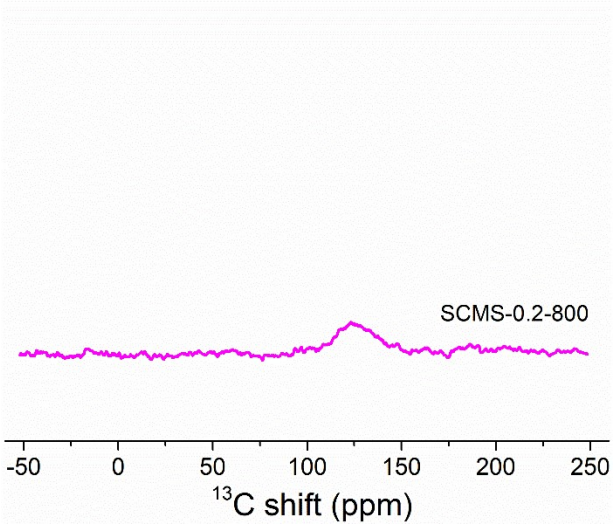

Figure S3. ^{13}C CP-MAS spectra of SCMS-0.2-800.

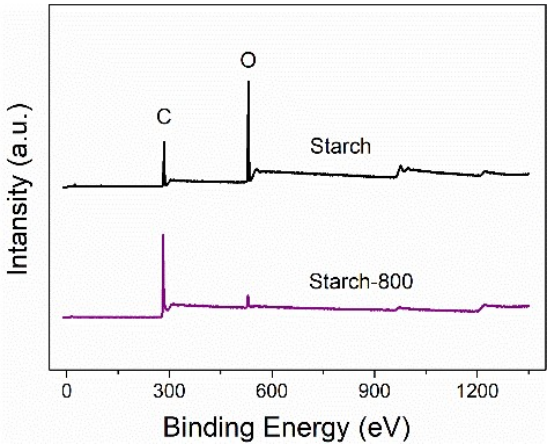

Figure S4. Full survey XPS spectra of starch and Starch-800.

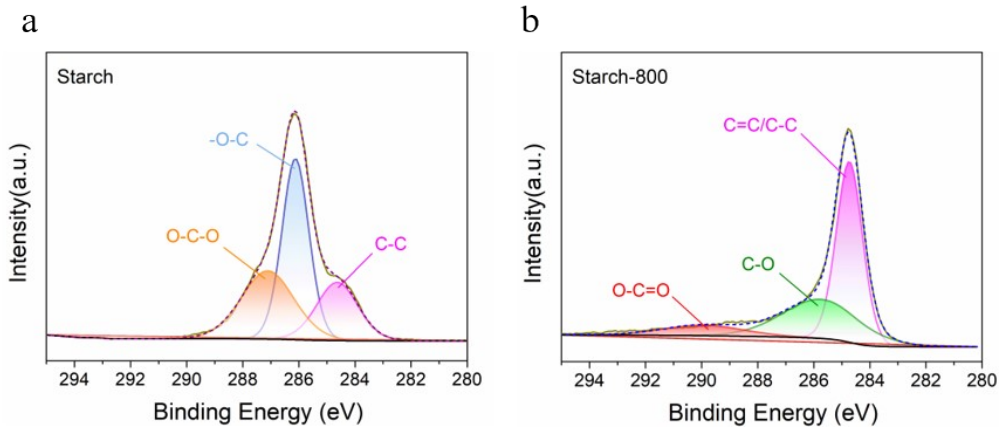

Figure S5. Deconvolution of C 1s spectra for (a) starch and (b) Starch-800.

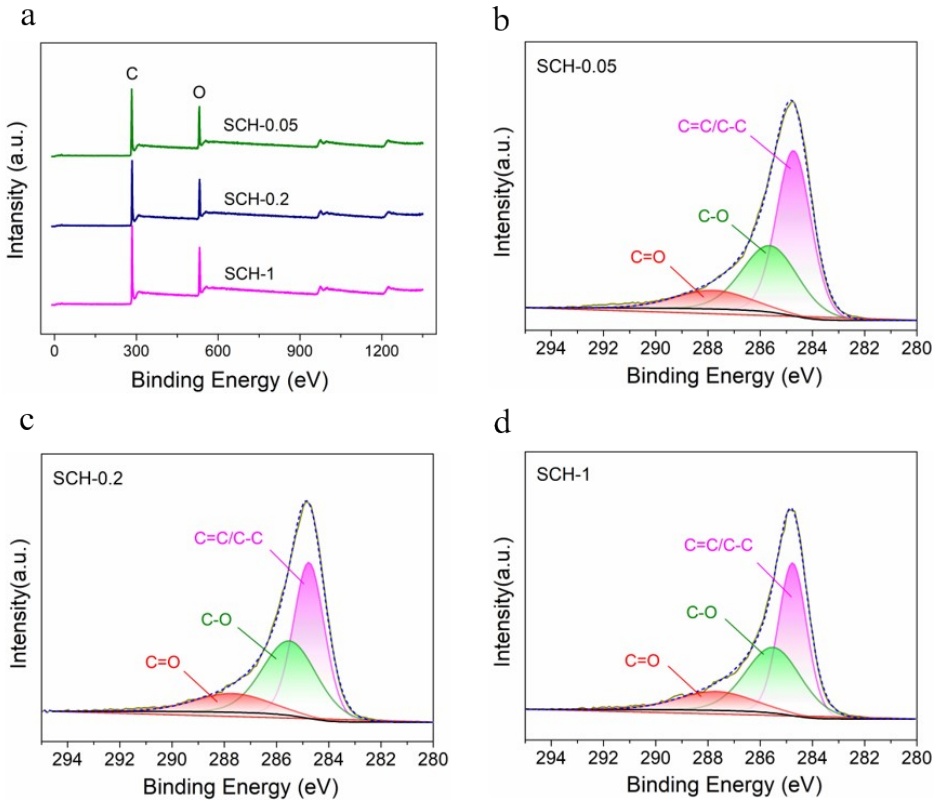

Figure S6. (a) Full survey XPS spectra of SCHs; (b-c) Deconvolution of C 1s spectra for SCHs.

XPS technique was applied to further reveal the composition and functionality of hydrochars (Figure S6). The obvious signals of C (284.8 eV) and O (532.8 eV) were observed without other impurities. The C_1 spectrum of SCH-*x* can be deconvoluted into three peaks corresponding to C=C/C-C (284.5 eV), C-O (285.7 eV) and C=O (287.5 eV).

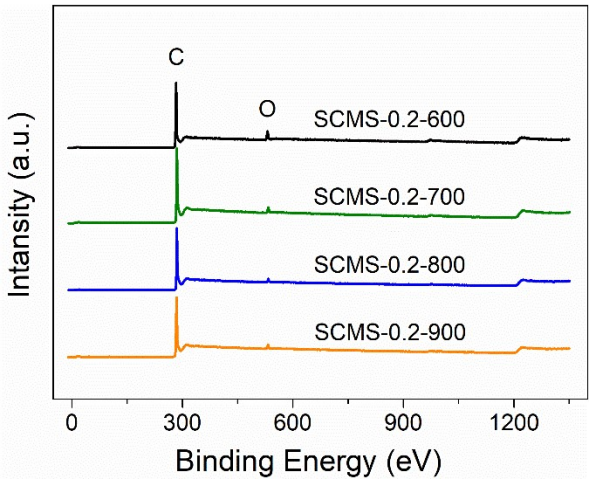

Figure S7. Full survey XPS spectra of SCMS-0.2-*y*.

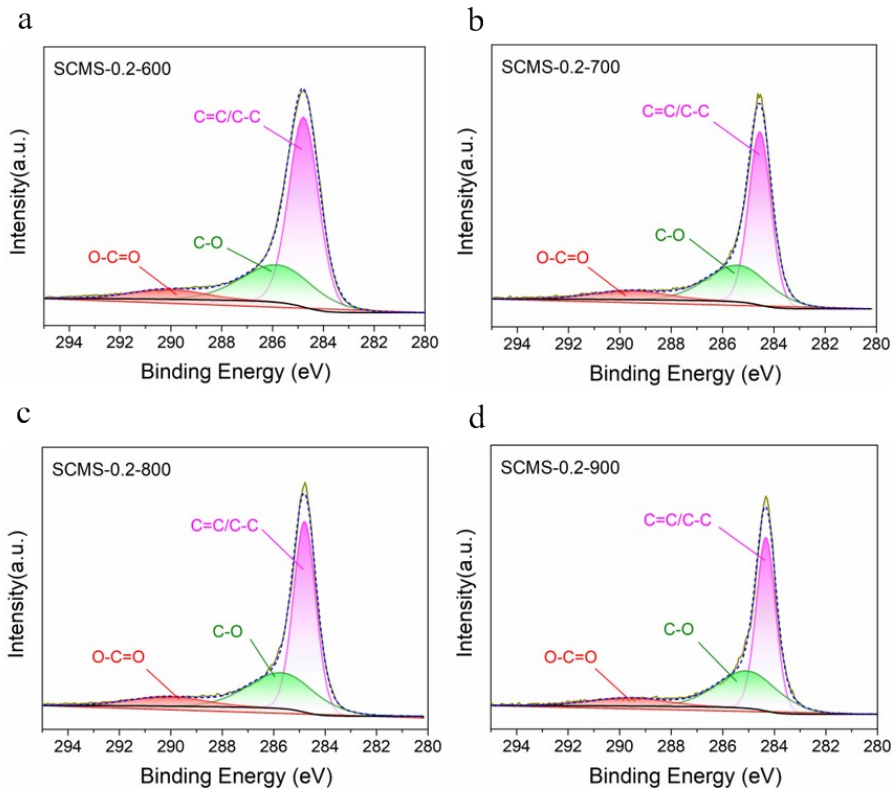

Figure S8. Deconvolution of C 1s spectra for SCMS-0.2-*y*.

When pyrolysis at high temperature is applied, It is noticed that with the attenuation of the C−O signals in the C1s envelopes, O-C=O (290.2 eV) bond signal showed up due to its high binding energy that is expected to be the partly remaining form of oxygen after annealing to high temperature (600-900 °C).[1]

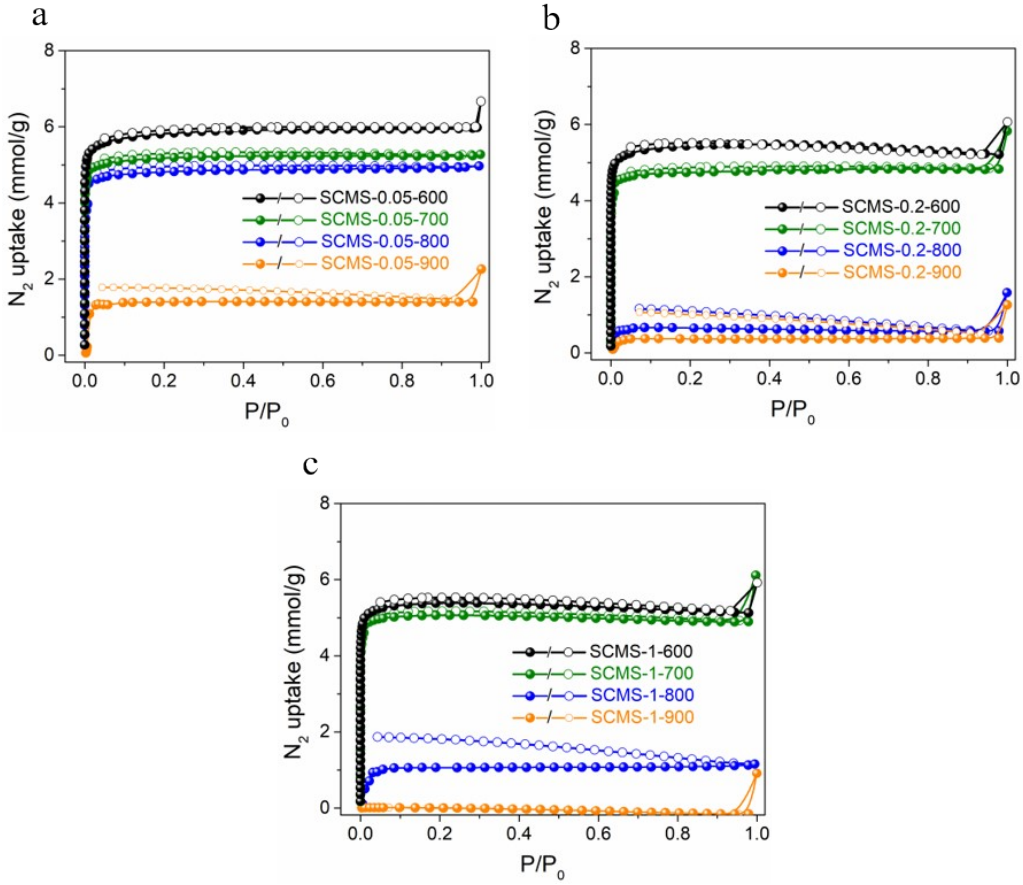

Figure S9. N_2 adsorption isotherms at 77 K on (a) SCMS-0.05- *y*; (b) SCMS-0.2-*y* and (c) SCMS-1- *y*.

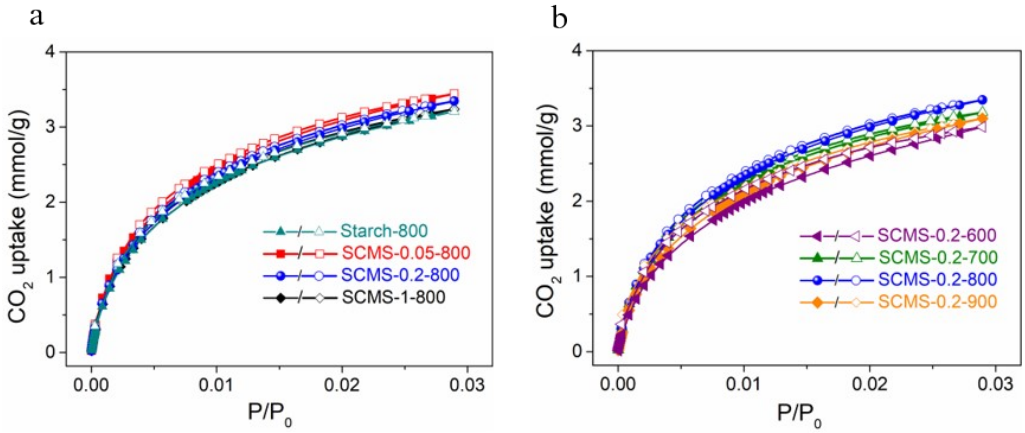

Figure S10. Adsorption isotherms of CO_2 on (a) Starch-800 and SCMS-*x*-800; (B) SCMS-0.2-*y*.

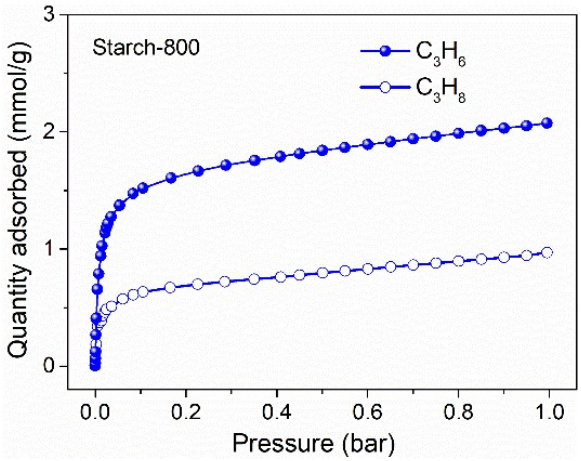

Figure S11. C_3H_6 and C_3H_8 adsorption isotherms of Starch-800 at 298 K and 0-1 bar. C_3H_6: solid circles, C_3H_8: empty circles

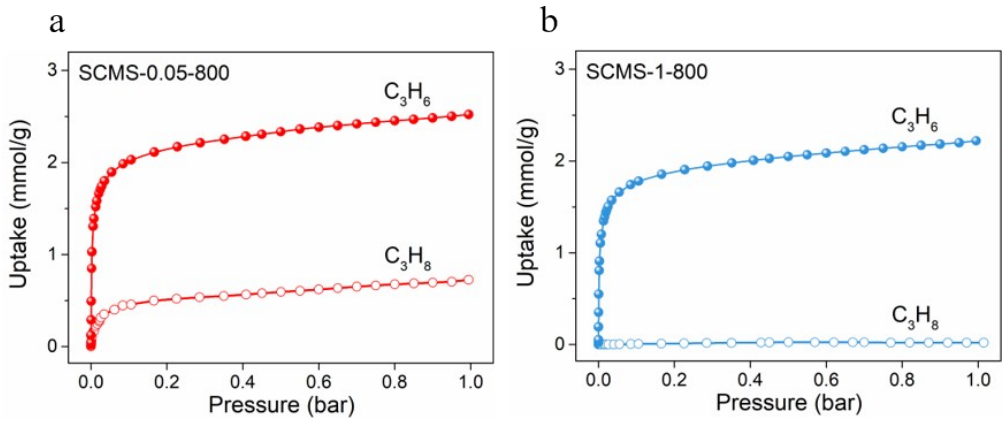

Figure S12. C_3H_6 and C_3H_8 adsorption isotherms of (a) SCMS-0.05-800 and (b) SCMS-1-800 at 298 K and 0-1 bar. C_3H_6: solid circles, C_3H_8: empty circles

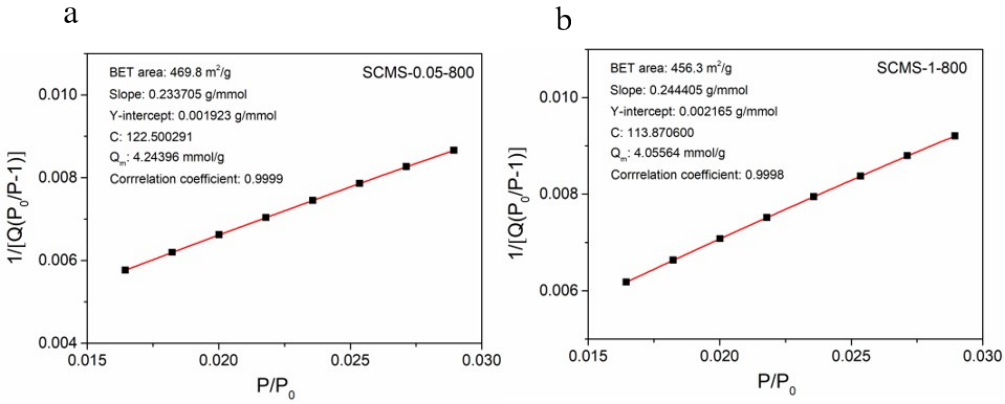

Figure S13. Surface area plot for SCMS-0.05-800 and SCMS-1-800.

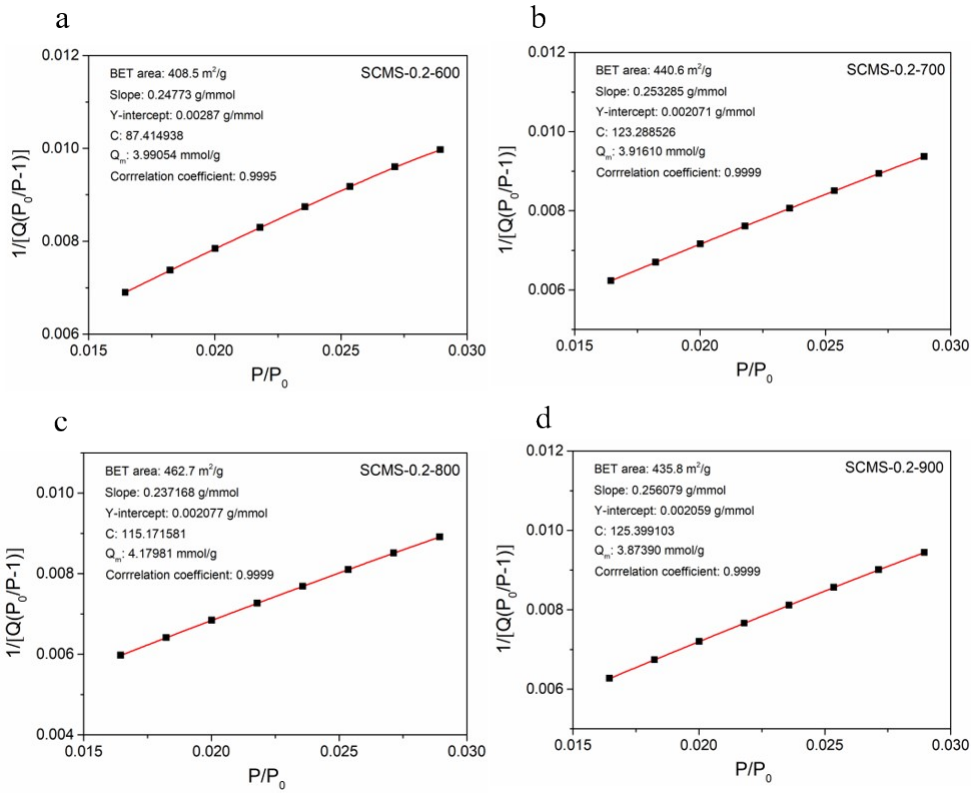

Figure S14. Surface area plot for SCMS-0.2-*y*.

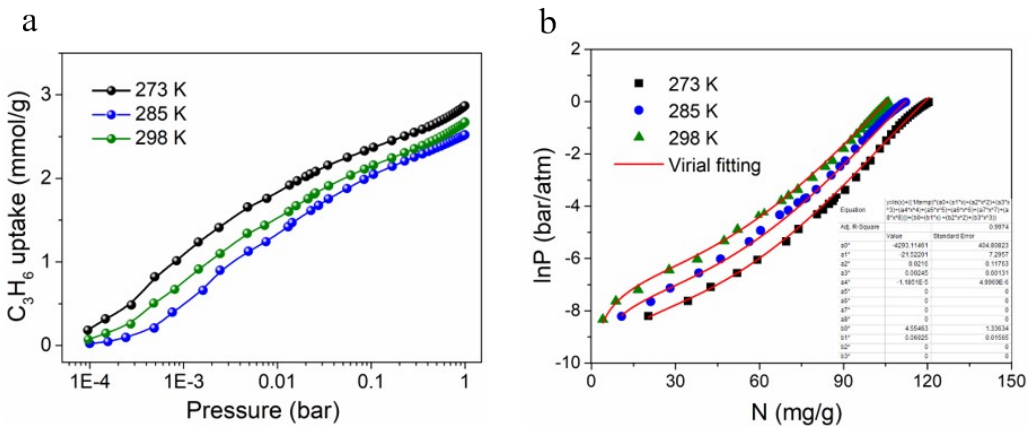

Figure S15. (a) C_3H_6 adsorption isotherms of SCMS-0.2-800 at three different temperatures and (b) Virial fitting of the C_3H_6 adsorption isotherms (points).

The isosteric heat of adsorption can be estimated from the adsorption isotherms at three different temperatures 273 K, 285 K and 298 K by using the Virial equation:[2]

$$lnP = lnN + 1/T\sum_{i=o}^{m} a_i N_i + \sum_{j=o}^{n} b_j N_j$$

Here, P refers to the pressure (bar), N is the amount absorbed (mmol/g), T is the temperature (K), a_i and b_j are Virial coefficients, and m, n represent the number of coefficients required to adequately describe the isotherms. The values of the Virial coefficients a_0 through a_m were then used to calculate the isosteric heat of absorption using the following expression:

$$Q_{st} = -R\sum_{i=o}^{m} a_i N_i$$

Where the Q_{st} is denoted as the coverage-dependent isosteric heat of adsorption, R refers to the ideal gas constant. The heat enthalpy of C_3H_6 is determined using the isotherms data in the pressure range from 0-1 bar (at 273 to 298 K).

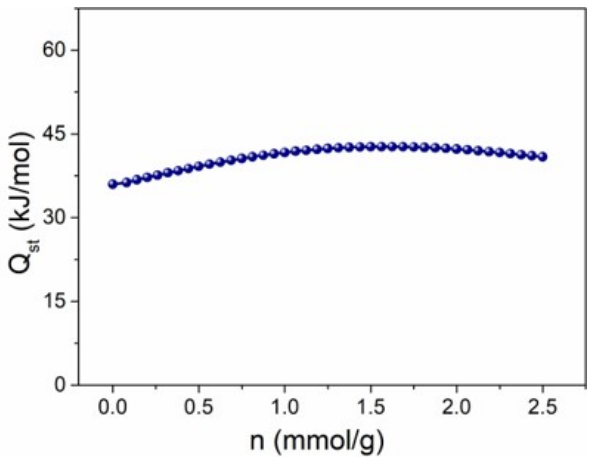

Figure S16. Heat of adsorption for C_3H_6 on SCMS-0.2-800.

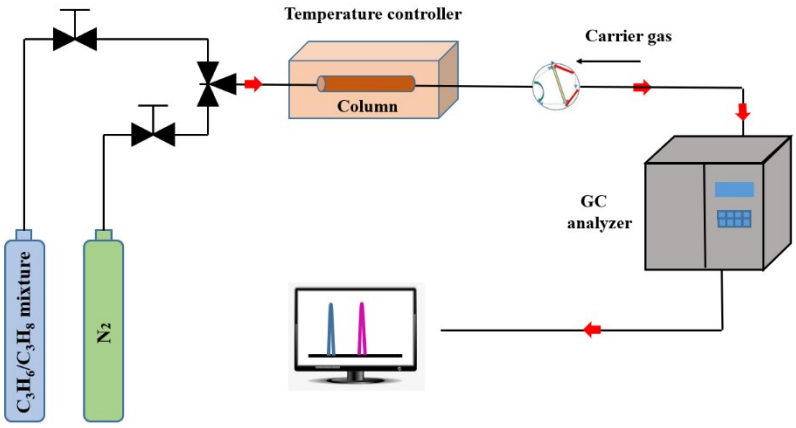

Figure S17. Schematic illustration of the apparatus for the gas breakthrough tests.

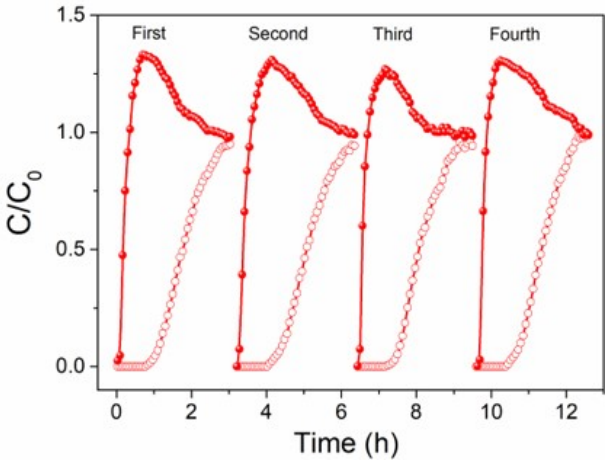

Figure S18. Breakthrough cycling test of SCMS-0.2-800. C_3H_6: solid circles, C_3H_8: empty circles.

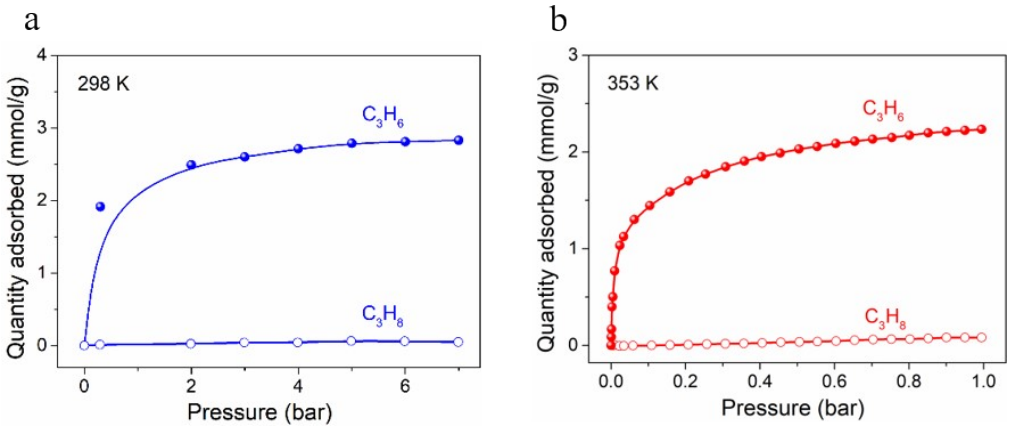

Figure S19. C_3H_6 and C_3H_8 adsorption isotherms of SCMS-0.2-800 at (a) 298 K and 0-8 bar; (b) 353 K and 0-1 bar. C_3H_6: solid circles, C_3H_8: empty circles

Supporting Tables

Table S1. Elemental compositions of SCHs from elemental analysis.

Samples	C%	O%	H%
SCH-0.05	69.37	26.50	4.13
SCH-0.2	68.44	27.28	4.28
SCH-1	67.55	28.08	4.37

Table S2. Comparison of C_3H_6 and C_3H_8 uptake of top-performing adsorbents at 1 bar and 298 K.

	Materials	C_3H_6 uptake (mmol/g)	C_3H_8 uptake (mmol/g)	Uptake ratio of C_3H_6/C_3H_8	Ref
MOFs	KAUST-7	1.41	~0	∞	3
	Y-abtc	1.95	~0	∞	4
	$Zn_3(OH)_2$(pzdc)(atz)	2.08	~0	∞	5
	Co-gallate	1.79	0.14	12.78	6
	Co(AIP)$(BPY)_{0.5}$	1.99[a]	0.48[a]	4.14[a]	7
	CPL-1	1.82	0.29	6.28	8
	AGTU-3a	1.22	0.46	2.65	9
	$Zn_2(5\text{-aip})_2$(bpy)	1.91	0.76	2.51	10
	SIFSIX-2-Cu-i	2.65	1.67	1.59	11
	$ZnAtzPO_4$	2.13	1.19	1.79	12
Zeolite	Zeolite 13X	3.44[b]	3.03[b]	1.14[b]	13
carbons	SAM-HCP-Ag-3	1.75	0.5	3.50	14
	MC-wiggle	2.6	1.5	1.7	15
	SC-K	2.20	0.41	5.37	16
	SCMS-0.05-800	**2.52**	**0.73**	**3.45**	**This work**
	SCMS-0.2-800	**2.54**	**0.08**	**31.75**	**This work**
	SCMS-1-800	**2.22**	**0.02**	**111**	**This work**
	SCMS-0.2-700	**2.24**	**1.69**	**1.33**	**This work**
	SCMS-0.2-900	**1.81**	**0.05**	**36.2**	**This work**

[a]: The experiment condition is 273 K and 100 kPa. [b]: The test temperature is 323 K.

Table S3. Textural properties of SCMS-0.2-*y* samples.

Samples	Micropore volume[a] (cm^3/g)
SCMS-0.2-600	0.220
SCMS-0.2-700	0.224
SCMS-0.2-800	0.238
SCMS-0.2-900	0.221

[a]: Micropore volume given by CO_2 adsorption data based on Dubinin−Radushkevich (D–R) equation

References

1. M. Acik, G. Lee, C. Mattevi, M. Chhowalla, K. Cho and Y. J. Chabal, *Nat. Mater*, 2010, **9**, 840-845.
2. L. Li, R.-B. Lin, R. Krishna, H. Li, S. Xiang, H. Wu, J. Li, W. Zhou and B. Chen, *Science*, 2018, **362**, 443-+.
3. A. Cadiau, K. Adil, P. M. Bhatt, Y. Belmabkhout and M. Eddaoudi, *Science*, 2016, **353**, 137-140.
4. H. Wang, X. Dong, V. Colombo, Q. Wang, Y. Liu, W. Liu, X. L. Wang, X. Y. Huang, D. M. Proserpio and A. Sironi, *Adv. Mater.*, 2018, **30**, 1805088.
5. X.-W. Zhang, D.-D. Zhou and J.-P. Zhang, *Chem*, 2021, DOI: https://doi.org/10.1016/j.chempr.2020.12.025.
6. B. Liang, X. Zhang, Y. Xie, R.-B. Lin, R. Krishna, H. Cui, Z. Li, Y. Shi, H. Wu, W. Zhou and B. Chen, *J. Am. Chem. Soc.*, 2020, **142**, 17795-17801.
7. H. Wu, Y. Yuan, Y. Chen, F. Xu, D. Lv, Y. Wu, Z. Li and Q. Xia, *AlChE J.*, 2020, **66**.
8. Y. Chen, Z. Qiao, D. Lv, C. Duan, X. Sun, H. Wu, R. Shi, Q. Xia and Z. Li, *Chem. Eng. J.*, 2017, **328**, 360-367.
9. Z. Chang, R.-B. Lin, Y. Ye, C. Duan and B. Chen, *J. Mater. Chem. A*, 2019, **7**, 25567-25572.
10. Y. Chen, H. Wu, D. Lv, N. Yuan, Q. Xia and Z. Li, *Sep. Purif. Technol.*, 2018, **204**, 75-80.
11. X. Wang, P. Zhang, Z. Zhang, L. Yang, Q. Ding, X. Cui, J. Wang and H. Xing, *Ind. Eng. Chem. Res*, 2020, **59**, 3531-3537.
12. Q. Ding, Z. Zhang, C. Yu, P. Zhang, J. Wang, L. Kong, X. Cui, C.-H. He, S. Deng and H. Xing, *AlChE J.*, 2021, **67**.
13. M. Campo, A. Ribeiro, A. Ferreira, J. Santos, C. Lutz, J. Loureiro and A. Rodrigues, *Sep. Purif. Technol.*, 2013, **103**, 60-70.
14. A. Stephenson, B. Li, L. Chen, R. Clowes, M. E. Briggs and A. I. Cooper, *J. Mater. Chem. A*, 2019, **7**, 25521-25525.
15. Y.-F. Yuan, Y.-S. Wang, X.-L. Zhang, W.-C. Li, G.-P. Hao, L. Han and A.-H. Lu, *Angew. Chem. Int. Ed.*, 2021, DOI: https://doi.org/10.1002/anie.202106523
16. S. Du, X. Wang, J. Huang, K. Kent, B. Huang, I. Karam, Z. Li and J. Xiao, *AlChE J.*, e17285.